

## RAPIDITY DEPENDENCE OF IDENTIFIED HADRON PRODUCTION IN d+Au COLLISIONS AT $\sqrt{s_{NN}} = 200$ GeV

HONGYAN YANG, for the BRAHMS Collaboration

*Department of Physics and Technology, University of Bergen, Norway*  
*hongyan.yang@ift.nib.no*

(Received November 15, 2005)

*Abstract.* We present the transverse momentum spectra for identified hadrons in d+Au collisions at  $\sqrt{s_{NN}} = 200$  GeV at  $\eta = 0, 1, 3, 2$ . The ratios  $R_{CP}$  of the identified hadron production in central (0–20%) and the semi-central (30–50%) d+Au collisions to the more peripheral (60–80%) ones, scaled by the number of binary collisions in different centrality classes, and the net protons'  $dN/dy$  at different rapidities in different centrality classes are presented.

*Key words:* rapidity dependence, identified hadrons, net protons.

### 1. INTRODUCTION

The d+Au collision at RHIC is an ideal experimental method to disentangle initial and final state effects in heavy-ion collisions, because compared to Au+Au system, d+Au collisions provide an important system to study the initial state effect since one does not expect the final state interactions to play a dominant role in such a small system, the effects of the initial stages remain mostly unchanged till the measurement is performed [1]. It is interesting to study the rapidity dependence of the identified hadrons production, especially the measurement on the net-protons' yield in the d+Au system might shed light on the baryon transport mechanism in the heavy ion collisions, which enable us understand the high energy collision scenarios better [2, 3].

### 2. THE BRAHMS EXPERIMENT AND PARTICLE IDENTIFICATION

BRAHMS, the **B**road **R**ange **H**adron **M**agnetic **S**pectrometers, is one of the four detectors at RHIC, located at 2 o'clock experimental hall of the RHIC collider. It has two rotatable magnetic spectrometers with particle identification capabilities



for hadrons, which gives the unique capability to study particle production in a broad range of both transverse momenta and rapidities.

The reaction centrality is determined by using a geometry weighted average of two global subsystems, the SiMA (Si Multiplicity Array) and the TMA (Tile Multiplicity Array) detectors, which select a fraction of events with a certain multiplicity within the pseudo-rapidity ranges of both multiplicity detectors.

The purpose of the mid-rapidity spectrometer (MRS) is to detect and identify the particles emitted at mid-rapidity. Particles at forward rapidities are detected by the Forward Spectrometer (FS). Both spectrometers have dipole magnets with tracking chambers located on each side of the magnet gaps. BRAHMS uses the Time-of-Flight (TOF) technique in both spectrometers, and a Ring Imaging Čerenkov (RICH) detector at the back of the FS for the identification of particles with high momentum. The left panel of the Fig. 1 shows the PID performance by time-of-flight wall (TOFW) achieved in MRS in d+Au data: a  $2\text{-}\sigma$  cut was implemented on  $\Delta(1/\beta)$ , which stands for the difference between the theoretical value  $1/\beta$  and the experimental measurement. In MRS, pions and kaons can be separated up to 1.6 GeV/c in momentum by the TOFW. The identification for pions and kaons is extended up to 25–30 GeV/c in FS by the RICH: a  $2\text{-}\sigma$  cut on the masses for each species was used, see the right panel of the Fig. 1. Details on the BRAHMS detector system can be found in Ref. [4].

### 3. DATA ANALYSIS AND PRELIMINARY RESULTS

The differential invariant cross-sections for identified hadrons, namely  $\pi^\pm$ ,  $K^\pm$  and  $p/\bar{p}$  are shown in Fig. 2. The data has been corrected for the spectrometer acceptance, tracking and PID efficiencies, in-flight decay and multiple scattering. The details for the method can be found in Ref. [5].

The ratio  $R_{CP}$  for the identified particles is defined as the yields from a given centrality class (0–20%, or 30–50%) divided by the yields from more peripheral collisions (60–80%), scaled by the mean number of binary collisions in each centrality bin, namely

$$R_{CP} = \frac{\langle N_{bin}^{Peripheral} \rangle d^2 N^{Central} / dp_T dy}{\langle N_{bin}^{Central} \rangle d^2 N^{Peripheral} / dp_T dy}. \quad (1)$$

By assuming that the nuclear modification is relatively small in the peripheral collisions, the deviation from unity of the  $R_{CP}$  is dominated by the nuclear effects in the more central collisions, which enable us to study the nuclear modification

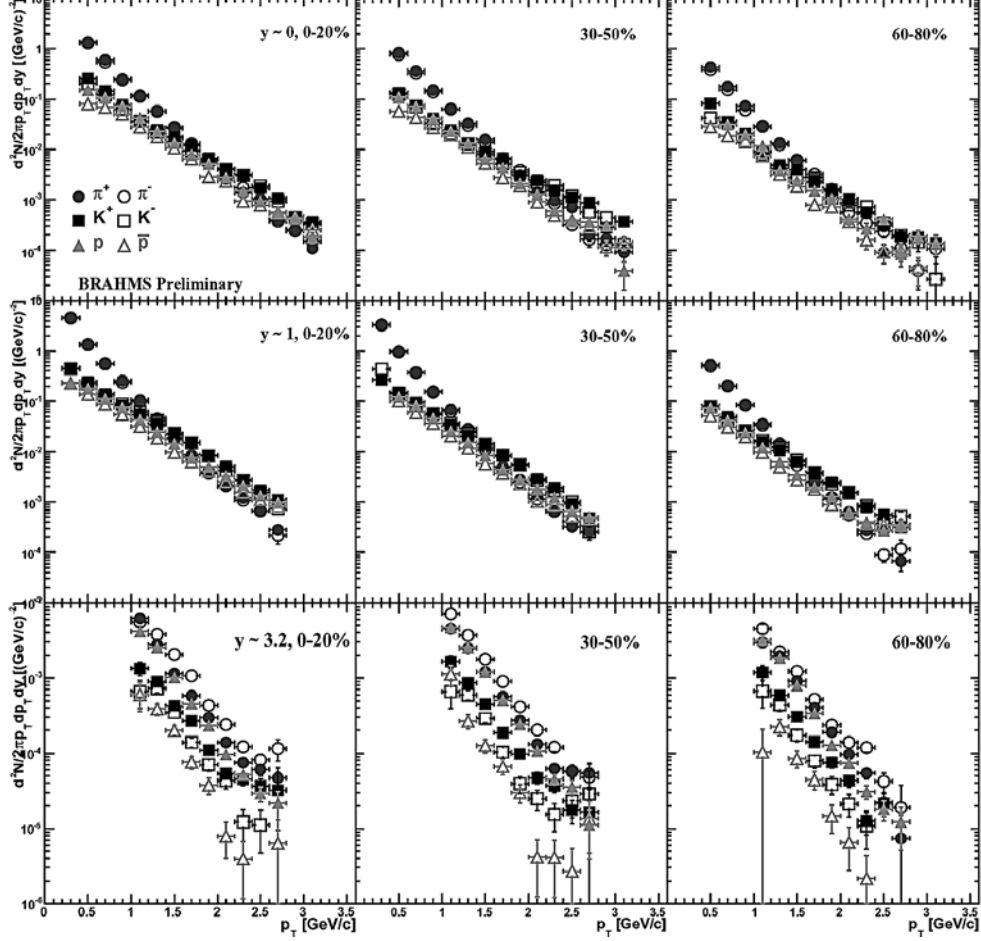


Fig. 2 – Differential invariant  $p_T$  spectra of identified particles at different rapidity and different centrality intervals.

independent of the p+p reference spectra. The averaged numbers of binary collisions used in our analysis are  $N_{bin}^{0-20\%} = 13.6 \pm 0.3$ ,  $N_{bin}^{30-50\%} = 7.9 \pm 0.4$  and  $N_{bin}^{60-80\%} = 3.3 \pm 0.4$ .

The evolution of  $R_{CP}$  with rapidity for identified particles is shown in Fig. 3. At mid-rapidity, the central-to-peripheral ratio is slightly larger than the semi-central-to-peripheral ratio for each identified particle specie, with very similar behavior to what was observed for that of the un-identified hadrons, suggesting the increased role of Cronin multiple scattering effects [6] in the more violent collisions. At forward rapidity,  $R_{CP}$  is very much suppressed in both cases, and no dependence on hadron specie is observed.

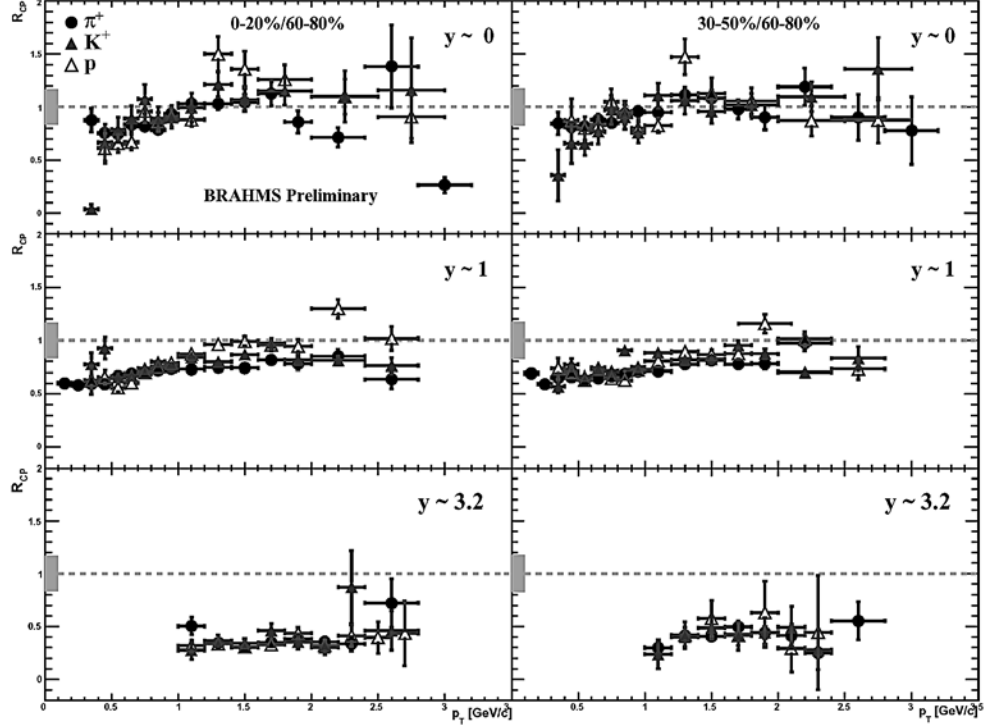


Fig. 3 –  $R_{CP}$  as a function of  $p_T$  for identified hadrons at different rapidity, and comparisons of the ratio of central (0–20%) to peripheral (60–80%) and semi-central (30–50%) to peripheral are shown. Errors shown here are statistical only, and the grey bands around 1.0 are the systematic errors caused by the uncertainties of  $N_{bin}$ .

Rapidity densities  $dN/dy$  are obtained by integrating the particle spectra over the full  $p_T$  range. Due to the lack of data at very low and high  $p_T$ , spectra are fitted by functions which describe them well. The fit function is then used to extrapolate to regions outside the acceptance. The protons spectra for different centrality classes, are fitted with the Boltzmann function in  $m_T$ , *i.e.*  $\sim m_T \exp[-(m_T - m)/T]$ , which describes the particle distribution emitted from a classical thermalized source at temperature  $T$ . Fig. 4 shows the rapidity density  $dN_{net}/dy$  of net-protons. From the centrality dependence of net-proton distribution in d+Au collisions, we can see that in the central and semi-central collisions, the net-proton yield increases when going to mid-rapidity from forward rapidity. But in the most peripheral collisions, the rapidity density distribution of the net-protons increases when going to both forward and mid-rapidity side from  $y \sim 1.0$ . The asymmetric net-proton rapidity density distribution in central events, can be understood as a strong baryon source on the gold fragmentation side and a weak one on the deuteron side.

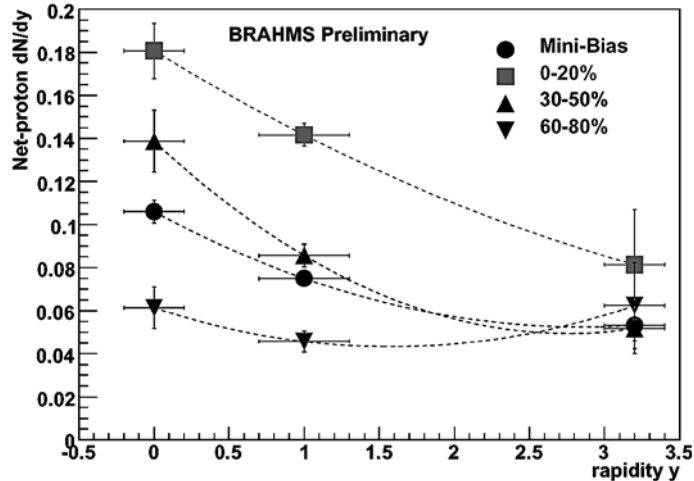


Fig. 4 – Rapidity density distribution for net-proton  $dN/dy$  in d+Au collisions. Errors are statistical only, and the dashed curves in the figure are just to guide the eye.

#### 4. DISCUSSIONS

In d+Au collisions, the Cronin effect at mid-rapidity is observed for pions, kaons and protons. The  $R_{CP}$  shows a suppression at forward rapidities for all species, which is consistent with what we have seen before for charged hadrons [7]. As has been discussed in Ref. [8], the peripheral Au+Au collisions are not equivalent to the p+p collisions, *i.e.* the  $R_{CP}$  for 0–10%/40–60% is more suppressed than  $R_{AA}$  in central Au+Au (0–10%) collisions. The d+Au data have been compared to a pQCD model where charged hadron spectra have been calculated to leading order, using standard fragmentation functions and shadowing parametrizations, to study how modifications to nuclear parton distributions affect production of high- $p_T$  hadrons in d+Au collisions. The  $R_{CP}$  measured by BRAHMS agree qualitatively with the model calculations at the same momentum region at mid-rapidity. However, at forward rapidity, the suppression in  $R_{CP}$  observed experimentally is very different from the model results. The rapidity density distribution of net-proton decreases significantly as  $y$  increases for central collision, while the increasing trend in the net-proton rapidity density in the peripheral collision was seen. The tendency of the production of net-proton rapidity density is consistent with the result by NA35 at SPS energies [10].

*Acknowledgements.* This work was supported by the Division of Nuclear Physics of the Office of Science of the U.S. Department of Energy, the Danish Research Council, the Research Council of Norway, the Jagiellonian University Grants, and the Romanian Ministry of Research.

## REFERENCES

1. L. McLerran and R. Venugopalan, Phys. Rev. **D 49**, (1994) 2233; Phys. Rev. **D 59**, (1999) 094002; E. Iancu, A. Leonidov and L. D. McLerran, Nucl. Phys. **A 692**, (2001) 583, and references therein.
2. F. Videback, O. Hansen, Physical Review **C 52**, (1995) 2684.
3. P. Christiansen, Ph.D Dissertation, Copenhagen University, May 2003.
4. M. Adamczyk *et al.*, [BRAHMS Collaboration], Nucl. Inst. Meth. **A 499**, (2003) 437.
5. D. Ouerdane, Ph.D Dissertation, Copenhagen University, August 2003.
6. J. W. Cronin, H. J. Frisch, M. J. Shochet *et al.*, Phys. Rev. D **11**, (1975) 3105.
7. I. Arsene *et al.*, [BRAHMS Collaboration], Phys. Rev. Lett. **93**, (2004) 242303.
8. P. Staszel for the BRAHMS Collaboration, proceeding for the Quark Matter Conference, Budapest, 2005.
9. R. Vogt, hep-ph/0405060, Phys. Rev. **C** in print.
10. T. Alber *et al.*, [NA35 Collaboration], Eur. Phys. J. **C 2**, (1998) 643.



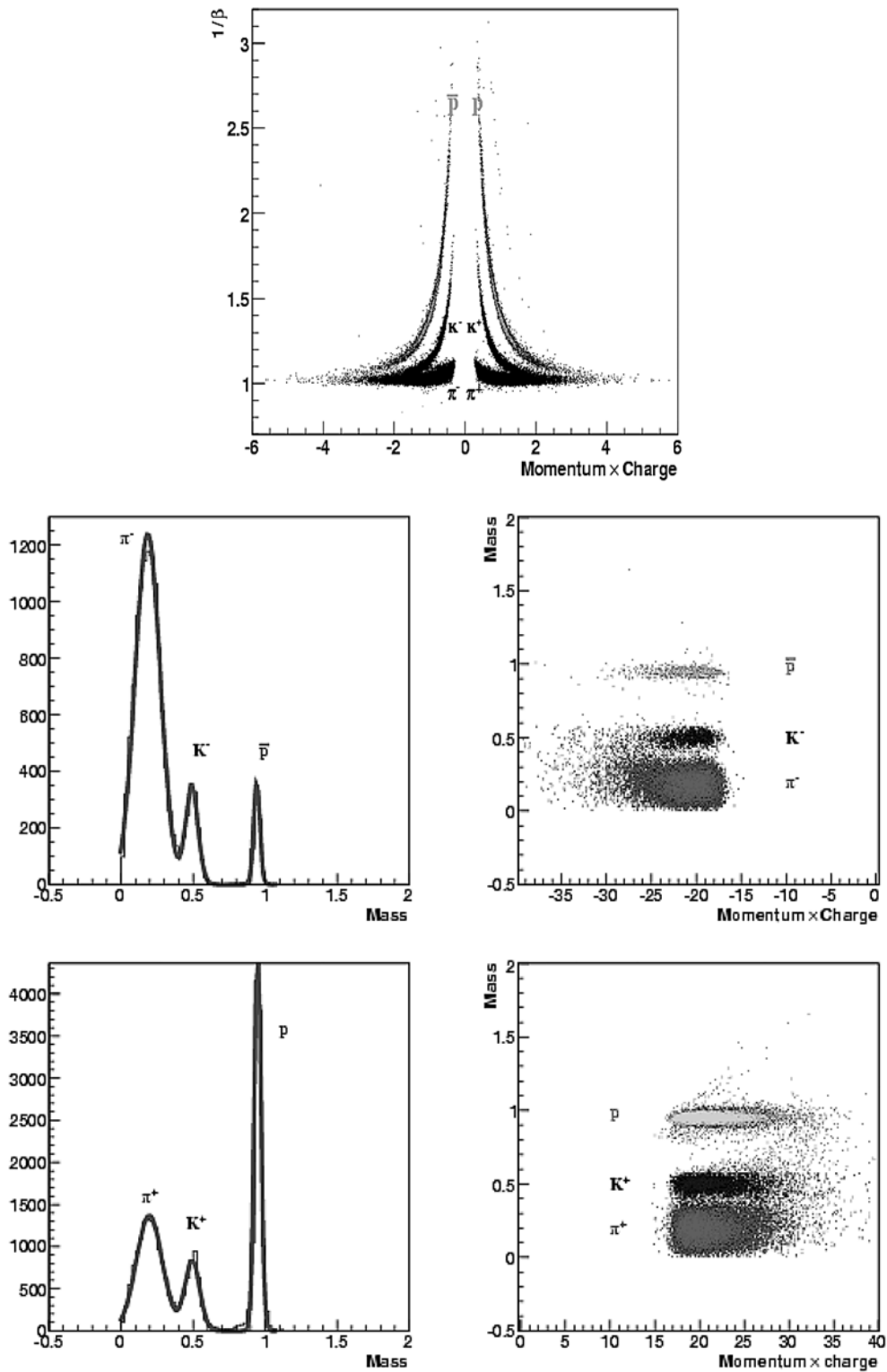


Fig. 1 – Left panel: particle identification in the MRS using TOFW, in which  $1/\beta = \sqrt{1 + m^2/p^2}$ , right panel: particle identification in the FS by RICH, the hadron mass ( $\text{GeV}/c^2$ ) vs. momentum  $\times$  charge ( $\text{GeV}/c$ ) were used. Right-upper and right-lower plots stand for the settings at 4 degree with A and B polarities correspondingly under full magnetic field.